Reduced Threshold for Luminal Ca^{2+} Activation of RyR1 Underlies a Causal Mechanism of Porcine Malignant Hyperthermia*

Dawei Jiang[‡1], **Wenqian Chen**[‡1], **Jianmin Xiao**[‡], **Ruiwu Wang**[‡], **Huihui Kong**[‡], **Peter P. Jones**[‡], **Lin Zhang**[‡], **Bradley Fruen**[§], and **S. R. Wayne Chen**[‡2]

From the [‡]*Libin Cardiovascular Institutes of Alberta, Departments of Physiology and Biophysics and Biochemistry and Molecular Biology, University of Calgary, Calgary, Alberta T2N 4N1, Canada and the* [§]*Department of Biochemistry, Molecular Biology and Biophysics, University of Minnesota, Minneapolis, Minnesota 55455*

Naturally occurring mutations in the skeletal muscle Ca^{2+} release channel/ryanodine receptor RyR1 are linked to malignant hyperthermia (MH), a life-threatening complication of general anesthesia. Although it has long been recognized that MH results from uncontrolled or spontaneous Ca^{2+} release from the sarcoplasmic reticulum, how MH RyR1 mutations render the sarcoplasmic reticulum susceptible to volatile anesthetic-induced spontaneous Ca^{2+} release is unclear. Here we investigated the impact of the porcine MH mutation, R615C, the human equivalent of which also causes MH, on the intrinsic properties of the RyR1 channel and the propensity for spontaneous Ca^{2+} release during store Ca^{2+} overload, a process we refer to as store overload-induced Ca^{2+} release (SOICR). Single channel analyses revealed that the R615C mutation markedly enhanced the luminal Ca^{2+} activation of RyR1. Moreover, HEK293 cells expressing the R615C mutant displayed a reduced threshold for SOICR compared with cells expressing wild type RyR1. Furthermore, the MH-triggering agent, halothane, potentiated the response of RyR1 to luminal Ca^{2+} and SOICR. Conversely, dantrolene, an effective treatment for MH, suppressed SOICR in HEK293 cells expressing the R615C mutant, but not in cells expressing an RyR2 mutant. These data suggest that the R615C mutation confers MH susceptibility by reducing the threshold for luminal Ca^{2+} activation and SOICR, whereas volatile anesthetics trigger MH by further reducing the threshold, and dantrolene suppresses MH by increasing the SOICR threshold. Together, our data support a view in which altered luminal Ca^{2+} regulation of RyR1 represents a primary causal mechanism of MH.

Malignant hyperthermia (MH)[3] is an autosomal dominant, pharmacogenetic disorder of skeletal muscle. MH is triggered by volatile anesthetics (*e.g.* halothane) and depolarizing muscle relaxants and is characterized by muscle rigidity and a hypermetabolic state (1–5). MH also occurs in pigs, in which it is caused by stress and known as porcine stress syndrome (6, 7). A single point mutation, R615C, in the pig skeletal muscle ryanodine receptor RyR1 is responsible for all cases of porcine MH (6, 7). On the other hand, human MH has been linked to a large number of mutations in RyR1 (4, 5, 8). Some human RyR1 mutations have also been linked to central core disease, which is often associated with MH. Although the genetic basis of MH has been well defined, the molecular mechanisms by which RyR1 mutations confer MH susceptibility and volatile anesthetics and stress trigger MH are not completely understood.

The pig model has proven invaluable in investigating the molecular basis of MH, and these studies have consistently demonstrated that Ca^{2+} release from MH-susceptible (MHS) pig skeletal muscle or sarcoplasmic reticulum (SR) membrane vesicles is enhanced upon exposure to various stimuli (1, 4, 9–14). However, to date no clear mechanistic basis of this enhanced responsiveness of MHS RyR1 channels to stimuli has emerged. For example, some studies reported that this enhanced activity of MHS RyR1 channels was associated with changes in the apparent sensitivity of the channel to cytosolic Ca^{2+} or Mg^{2+}, whereas others found no marked difference in the apparent sensitivity to cytosolic Ca^{2+} activation between MHS and normal RyR1 channels (1, 13–20). Hence, the intrinsic properties of the RyR1 channel that are altered by the MH R615C mutation have remained undefined.

Increasing evidence has highlighted the importance not only of cytosolic Ca^{2+}, but also of luminal Ca^{2+}, in controlling the activity of the RyR channel (21–23). However, in comparison with the extensive investigations of the sensitivity of MHS RyR1 channels to cytosolic Ca^{2+} and Mg^{2+}, the effects of the MH R615C mutation on the luminal Ca^{2+} sensitivity of the channel remain largely unexplored. A notable exception is found among the earliest work investigating the effect of the MH R615C mutation on Ca^{2+} handling by isolated SR membranes (13, 24, 25). Nelson and colleagues (13, 24, 25) originally reported that the luminal Ca^{2+} load required to trigger spontaneous SR Ca^{2+}

release was markedly reduced in SR membranes isolated from MHS animals, suggesting that a defect in intraluminal Ca^{2+} regulation may underlie MH.

We have recently shown that disease-causing mutations in the cardiac ryanodine receptor RyR2 increase the sensitivity of the channel to activation by luminal Ca^{2+} and enhance the propensity for spontaneous Ca^{2+} release during store Ca^{2+} overload, a process we have termed store overload-induced Ca^{2+} release (SOICR) (26, 27). Interestingly, disease-linked RyR2 mutations are located in regions corresponding to the MH/central core disease mutation regions in RyR1 (28). This similar distribution suggests that disease-linked RyR2 and RyR1 mutations may exert similar effects on the intrinsic properties of the channel. To test this hypothesis, in the present study, we assessed the impact of the MH R615C mutation and the MH-triggering agent, halothane, on the response of RyR1 to luminal Ca^{2+} and the propensity for SOICR. We found that the R615C mutation and halothane potentiated luminal Ca^{2+} response and SOICR. On the other hand, dantrolene, the only treatment for MH, suppressed SOICR. We propose that a reduced threshold for SOICR as a result of augmented luminal Ca^{2+} activation of RyR1 represents a primary defect underlying the pathogenesis of MH.

EXPERIMENTAL PROCEDURES

Site-directed Mutagenesis—The R615C RyR1 MH mutation in the rabbit RyR1 cDNA was made by the PCR-based overlap extension method (29). The sequence of the PCR-amplified region was confirmed by DNA sequencing. The full-length RyR1 wt and R615C mutant cDNAs were subcloned into the mammalian expression vector pcDNA3.

Single Channel Recordings—Pig RyR1 wt and R615C mutant proteins were partially purified from normal and MHS pig SR microsomes by sucrose density gradient centrifugation. Heart phosphatidylethanolamine and brain phosphatidylserine (Avanti Polar Lipids), dissolved in chloroform, were combined in a 1:1 ratio (w/w), dried under nitrogen gas, and suspended in 30 μl of *n*-decane at a concentration of 12 mg lipid/ml. Bilayers were formed across a 250-μm hole in a Delrin partition separating two chambers. The trans chamber (800 μl) was connected to the head stage input of an Axopatch 200A amplifier (Axon Instruments, Austin, TX). The cis chamber (1.2 ml) was held at virtual ground. A symmetrical solution containing 250 mM KCl and 25 mM Hepes (pH 7.4), was used for all recordings, unless indicated otherwise. A 4-μl aliquot ($\approx$1 μg of protein) of the sucrose density gradient-purified wt or mutant RyR1 proteins was added to the cis chamber. Spontaneous channel activity was always tested for sensitivity to EGTA and Ca^{2+}. The chamber to which the addition of EGTA inhibited the activity of the incorporated channel presumably corresponds to the cytoplasmic side of the Ca^{2+} release channel. The direction of single channel currents was always measured from the luminal to the cytoplasmic side of the channel, unless mentioned otherwise. Recordings were filtered at 5,000 Hz. Data analyses were carried out using the pclamp 8.1 software package (Axon Instruments). Free Ca^{2+} concentrations were calculated using the computer program of Fabiato and Fabiato (30).

Generation of Stable, Inducible HEK293 Cell Lines—Stable, inducible HEK293 cell lines expressing RyR1 wt and the R615C mutant were generated using the Flp-In T-REx core kit from Invitrogen. Briefly, the full-length cDNA encoding the RyR1 wt or mutant channel was subcloned into the inducible expression vector, pcDNA5/FRT/TO (Invitrogen). Flp-In T-REx-293 cells were then co-transfected with the inducible expression vector containing the RyR1 wt or mutant cDNA and the pOG44 vector encoding the Flp recombinase in 1:5 ratios using the Ca^{2+} phosphate precipitation method. Transfected cells were washed with phosphate-buffered saline (137 mM NaCl, 8 mM Na$_2$HPO$_4$, 1.5 mM KH$_2$PO$_4$, 2.7 mM KCl) 1 day after transfection and allowed to grow for 1 more day in fresh medium. The cells were then washed again with phosphate-buffered saline, harvested, and plated onto new dishes. After the cells had attached ($\sim$4 h), the growth medium was replaced with a selective medium containing 200 μg/ml hygromycin (Invitrogen). The selective medium was changed every 3–4 days until the desired number of cells was grown. The hygromycin-resistant cells were pooled, aliquoted, and stored at -80 °C. These positive cells are believed to be isogenic, because the integration of the RyR1 cDNA is mediated by the Flp recombinase at a single target site. Each HEK293 cell line was tested for RyR1 expression using Western blotting analysis and immunocytofluorescence staining.

Single Cell Ca^{2+} Imaging (Cytosolic Ca^{2+})—Intracellular Ca^{2+} transients in stable inducible HEK293 cells expressing the RyR1 wt or the R615C mutant channels were measured using single-cell Ca^{2+} imaging and the fluorescent Ca^{2+} indicator dye fura-2 acetoxymethyl ester (AM) as described previously (26). Cells grown on glass coverslips for 24 h after induction by 1 mg/ml tetracycline (Sigma) were loaded with 5 μM fura-2 AM in Krebs-Ringer-Hepes (KRH) buffer (125 mM NaCl, 5 mM KCl, 1.2 mM KH$_2$PO$_4$, 6 mM glucose, 1.2 mM MgCl$_2$, 25 mM Hepes, pH 7.4) plus 0.02% pluronic F-127 (Molecular Probes) and 0.1 mg/ml bovine serum albumin for 20 min at room temperature. The coverslips were then mounted in a perfusion chamber (Warner Instruments, Hamden, CT) on an inverted microscope (Nikon TE2000-S) equipped with an S-Fluor 20$\times$/0.75 objective. The cells were continuously perfused with KRH buffer containing various concentrations of CaCl$_2$ (0.2–10 mM) at room temperature. 10 mM caffeine was applied at the end of each experiment to confirm the expression of active RyR1 channels. Time lapse images (0.33 frames s^{-1}) were captured and analyzed with the Compix Inc. Simple PCI6 software.

Single Cell Ca^{2+} Imaging (Luminal Ca^{2+})—To monitor PCI6 luminal Ca^{2+} transients in HEK293 cells, we used the Ca^{2+}-sensitive fluorescence resonance energy transfer (FRET)-based cameleon protein D1ER (31). Stable, inducible HEK293 cells expressing RyR1 wt or mutant channels were transfected using the Ca^{2+} phosphate precipitation method, with D1ER cDNA 24 h before the induction of RyR1 expression. The cells were perfused continuously with KRH buffer (125 mM NaCl, 5 mM KCl, 1.2 mM KH$_2$PO$_4$, 6 mM glucose, 1.2 mM MgCl$_2$, 25 mM Hepes, pH 7.4) containing various concentrations of CaCl$_2$ (0 or 5 mM) and tetracaine (1 mM) or caffeine (20 mM) at room temperature. The images were captured with Compix Inc. Simple PCI 6 software at 470- and 535-nm emission, with excitation at
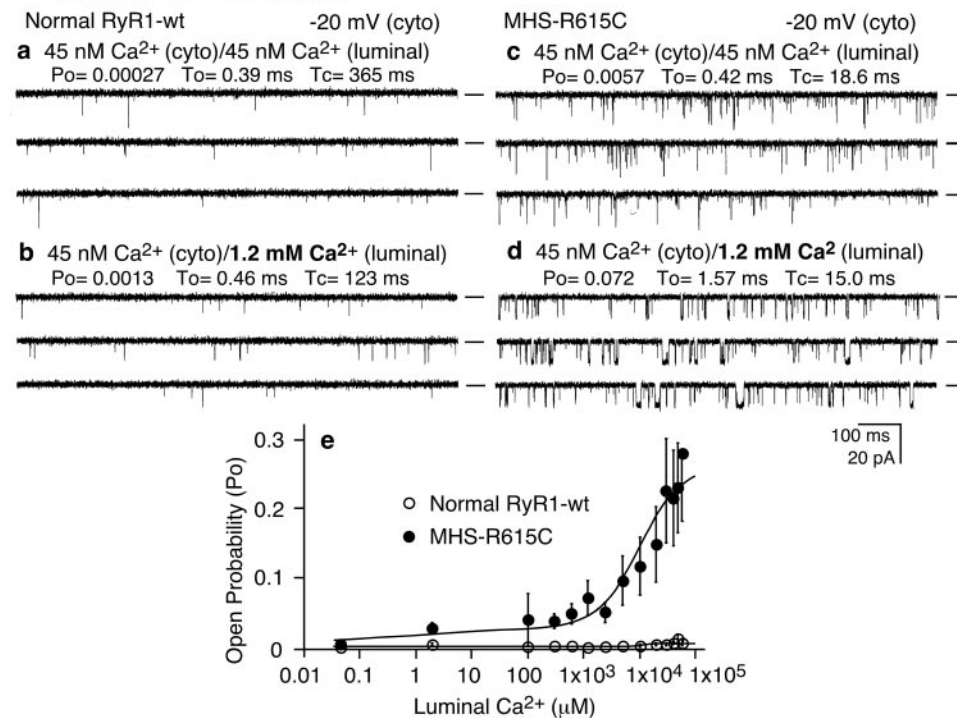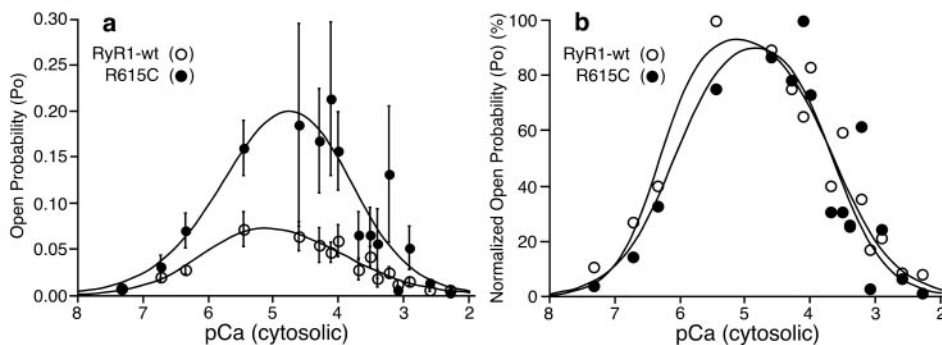
A Luminal Ca²⁺ Response

FIGURE 1. **Single RyR1 channels from normal and MHS pig SR differ in their responses to luminal Ca²⁺.** *A*, the activities of single RyR1 channel from normal (*panels a and b*) and MHS (*panels c and d*) pig skeletal muscle SR were recorded in a symmetrical recording solution containing 250 mM KCl and 25 mM Hepes (pH 7. 4) at a holding potential of −20 mV. The Ca²⁺ concentration on both the cytosolic and luminal sides of the channel was adjusted to ~45 nM (*panels a and c*). The luminal Ca²⁺ concentration was then increased to various levels by the addition of aliquots of CaCl₂ solution. Single-channel current traces at 1.2 mM luminal Ca²⁺ are shown (*panels b and d*). The relationships between P_o and luminal Ca²⁺ concentrations are shown in *panel e*. The data points are the means ± S.E. from 8 wt and 14 R615 single channels. Openings are downward. The open probability (P_o), arithmetic mean open time (T_o), and arithmetic mean closed time (T_c) are indicated on the *top* of each panel. *B*, the response of normal and MHS RyR1 channels to cytosolic Ca²⁺. The responses of normal (RyR1 wt) and MHS (R615C) to cytosolic Ca²⁺ were assessed using single channel recordings. The luminal Ca²⁺ concentration was kept at 45 nM. *Panel a* shows relationships between open probability (P_o) and cytosolic Ca²⁺ concentration (pCa) of single wt (*open circles*) and single R615C mutant (*solid circles*) channels. The normalized (100%) P_o-pCa relationships are shown in *panel b*. The data points shown are the means ± S.E. from 10 wt and 10 R615C mutant channels.

430 nm, every 2 s using an inverted microscope (Nikon TE2000-S) equipped with a S-Fluor 20×/0.75 objective. The amount of FRET was determined from the ratio of the emissions at 535 and 470 nm.

RESULTS

The Porcine MH R615C Mutation Enhances the Luminal Ca²⁺ Activation of Single RyR1 Channels—To directly assess the impact of the R615C mutation on luminal Ca²⁺ activation,

we incorporated single normal (RyR1 wt) and MHS (RyR1-R615C) RyR1 channels into planar lipid bilayers and examined their responses to increasing concentrations of luminal Ca²⁺. As shown in Fig. 1*A*, elevating the luminal Ca²⁺ concentration from ~45 nM to 50 mM had little effect on single wt channels but markedly activated single R615C mutant channels with an activation threshold of about 0.5 mM luminal Ca²⁺ (Fig. 1*A*, *panel e*). For instance, at 1.2 mM luminal Ca²⁺, the average open probability (P_o) for single R615C mutant channels was 0.070 ± 0.024 ($n = 14$) (Fig. 1*A*, *panel d*), which was significantly greater than that of single wt channels (0.001 ± 0.0004, $n = 8$) ($p < 0.05$) (Fig. 1*A*, *panel b*). These observations directly demonstrate that the R615C mutation enhances the response of the RyR1 channel to luminal Ca²⁺ activation.

The R615C Mutation Has Little Effect on the Cytosolic Ca²⁺ Dependence of Single RyR1 Channels—We next determined the response of wt and R615C to cytosolic Ca²⁺ using single channel recordings. As shown in Fig. 1*B*, both single wt and R615C channels were maximally activated by ~10 μM cytosolic Ca²⁺ with an activation threshold about ~100 nM and were completely inhibited by ~5 mM Ca²⁺. Although the extent of maximum activation of the R615C channels by cytosolic Ca²⁺ was greater than that of the wt channels (Fig. 1*B*, *panel a*), the cytosolic Ca²⁺ dependence of activation or inactivation of the wt and R615C channels was similar, as seen from the normalized Ca²⁺ responses (Fig. 1*B*, *panel b*). These observations indicate that the R615C mutation does not markedly alter the sensitivity of single RyR1 channels to cytosolic Ca²⁺ activation or inactivation.

Halothane Potentiates the Luminal Ca²⁺ Response of Single RyR1 Channels—The effect of halothane on the luminal Ca²⁺ activation of single RyR1 channels was also investigated (Fig. 2). A single R615C mutant channel exhibited little activity in the presence of 45 nM cytosolic and luminal Ca²⁺ (Fig. 2*A*). The addition of 600 μM luminal Ca²⁺ slightly activated the channel (Fig. 2*B*). A subsequent addition of 20 mM halothane to the
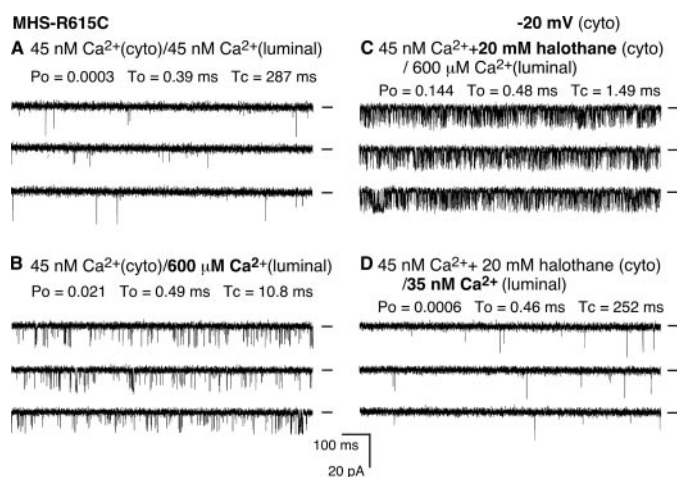
FIGURE 2. **Halothane potentiates the response of RyR1 to luminal Ca²⁺.** Single channel activities of the R615C mutant were recorded as described in the legend to Fig. 1. The Ca²⁺ concentration on both the cytosolic and luminal sides of the channel was adjusted to ~45 nM (A). The luminal Ca²⁺ concentration was then increased to 600 μM (B). C, single channel current traces after the addition of halothane to the cytosolic side of the channel. The luminal Ca²⁺ concentration was then reduced to ~35 nM in the continued presence of halothane (D). The holding potential was −20 mV, and the openings are downward.

cytosolic side of the channel markedly increased the channel activity (Fig. 2C). The average P_o after the addition of halothane was 0.176 ± 0.049 ($n = 6$) in the presence of 600 μM luminal Ca²⁺, which was significantly greater than that before the addition of halothane (0.030 ± 0.004) ($n = 6$) ($p < 0.03$). It should be noted that halothane has been shown to have little effect on the apparent affinity of EGTA for Ca²⁺ (32). Importantly, this halothane-induced enhancement was dependent on the presence of luminal Ca²⁺. Reducing the luminal Ca²⁺ from 600 μM to ~35 nM decreased the channel activity to the basal level (Fig. 2D). Similarly, halothane also activated single RyR1 wt channels in a luminal Ca²⁺-dependent manner (not shown). It should be noted that because of its highly volatile nature, the actual concentration of halothane in the bilayer recording solution would be much lower than that added to the chamber. Nevertheless, these data indicate that at low cytosolic Ca²⁺, halothane potentiates the response of RyR1 to luminal Ca²⁺.

Halothane and the R615C Mutation Enhance the Propensity for SOICR in HEK293 Cells—It has long been demonstrated that halothane induces spontaneous contracture in MHS muscle, but not in normal muscle in an external Ca²⁺-dependent manner (33), and that the halothane-induced spontaneous SR Ca²⁺ release is dependent on the SR Ca²⁺ load (34). To determine whether halothane and the R615C mutation also augment RyR1-mediated spontaneous Ca²⁺ release or SOICR in a nonmuscle environment, we generated stable, inducible HEK293 cell lines expressing wt or R615C. We have previously shown that elevated $[Ca^{2+}]_o$ induces SOICR in HEK293 cells expressing RyR2 (26, 27). Unlike RyR2-expressing cells, cells expressing RyR1 wt or the R615C mutant did not show SOICR in response to elevated $[Ca^{2+}]_o$ in the absence of stimuli (Fig. 3A, *panel b*). However, in the presence of low concentrations of halothane, elevated $[Ca^{2+}]_o$ triggered SOICR in both RyR1 wt- and R615C mutant-expressing HEK293 cells (Fig. 3A, *panels a*

and *b*). Analyzing a number of oscillating cells revealed that HEK293 cells expressing R615C displayed a greater propensity for SOICR than cells expressing wt (Fig. 3A, *panel b*). The frequency of Ca²⁺ oscillations in cells expressing the R615C mutant was also much higher than that in cells expressing wt (Fig. 3A, *panel c*). Similar results were obtained when halothane was replaced with caffeine (Fig. 3A, *panels d* and *e*). The parental HEK293 cells do not express a detectable level of RyRs (26, 35). These observations indicate that the MH R615C mutation, halothane, and caffeine can enhance the propensity for SOICR in a nonmuscle environment, suggesting that the response of RyR1 to Ca²⁺ overload is a major determinant of halothane- or caffeine-induced spontaneous Ca²⁺ release.

The R615C Mutation Reduces the Luminal Ca²⁺ Threshold at Which SOICR Occurs—To directly measure the luminal Ca²⁺ threshold at which SOICR occurs, we used a FRET-based endoplasmic reticulum (ER) Ca²⁺ sensor protein, D1ER (31), to monitor the ER luminal Ca²⁺ dynamics during store Ca²⁺ overload in HEK293 cells expressing RyR1 wt or R615C. As shown in Fig. 3B (*panels a* and *b*), elevated $[Ca^{2+}]_o$ increased the level of ER luminal Ca²⁺. When the luminal Ca²⁺ reached a threshold level, SOICR occurred, displaying as downward deflections in the FRET signal. SOICR was then suppressed by 1.0 mM tetracaine, an inhibitor of RyR1, to estimate the maximum luminal Ca²⁺ level. Caffeine (20 mM), an activator of RyR1, was then used to estimate the minimum luminal Ca²⁺ level by emptying the store. Fig. 3B (*panel c*) shows that the luminal Ca²⁺ threshold (percentage of maximum luminal Ca²⁺ store capacity) at which SOICR occurs is significantly lower in cells expressing R615C ($76.1 \pm 0.8\%$, $n = 243$) than in cells expressing wt ($89.5 \pm 1.0\%$, $n = 106$) ($p < 0.00001$) in the presence of 2 mM caffeine. There was no significant difference in the maximum luminal Ca²⁺ store capacity between the R615C-expressing cells ($105.5 \pm 6.2\%$) and the wt-expressing cells (100%) ($p = 0.25$), which was calculated by subtracting the minimum FRET signal (in the presence of 20 mM caffeine) from the maximum FRET signal (in the presence of 1 mM tetracaine). Similarly, the luminal Ca²⁺ threshold at which SOICR occurs is significantly lower in cells expressing R615C ($80.0 \pm 3.1\%$, $n = 107$) than in cells expressing wt ($93.2 \pm 0.8\%$, $n = 108$) ($p < 0.00001$) in the presence of 2 mM halothane. The resting luminal Ca²⁺ level in the presence of near 0 mM external Ca²⁺ and 2 mM caffeine is also lower in cells expressing R615C ($34.0 \pm 2.9\%$) than in cells expressing wt ($54.5 \pm 4.5\%$) ($p < 0.00001$). Similarly, the resting luminal Ca²⁺ level in the presence of near 0 mM external Ca²⁺ and 2 mM halothane is lower in cells expressing R615C ($62.8 \pm 3.3\%$) than in cells expressing wt ($81.5 \pm 2.4\%$) ($p < 0.00001$). Taken together, these data are consistent with those of single channel studies showing that the R615C mutation and halothane enhance the response of RyR1 to luminal Ca²⁺, leading to a reduced SOICR threshold and resting ER Ca²⁺ level.

Dantrolene Abolishes SOICR in HEK293 Cells Expressing RyR1-R615C but Not in Cells Expressing RyR2-N4104K—It has also long been shown that dantrolene suppresses caffeine- or halothane-induced spontaneous contracture in MHS muscle (36, 37) and that dantrolene inhibits spontaneous Ca²⁺ release from skeletal muscle SR but not from cardiac muscle SR (38).
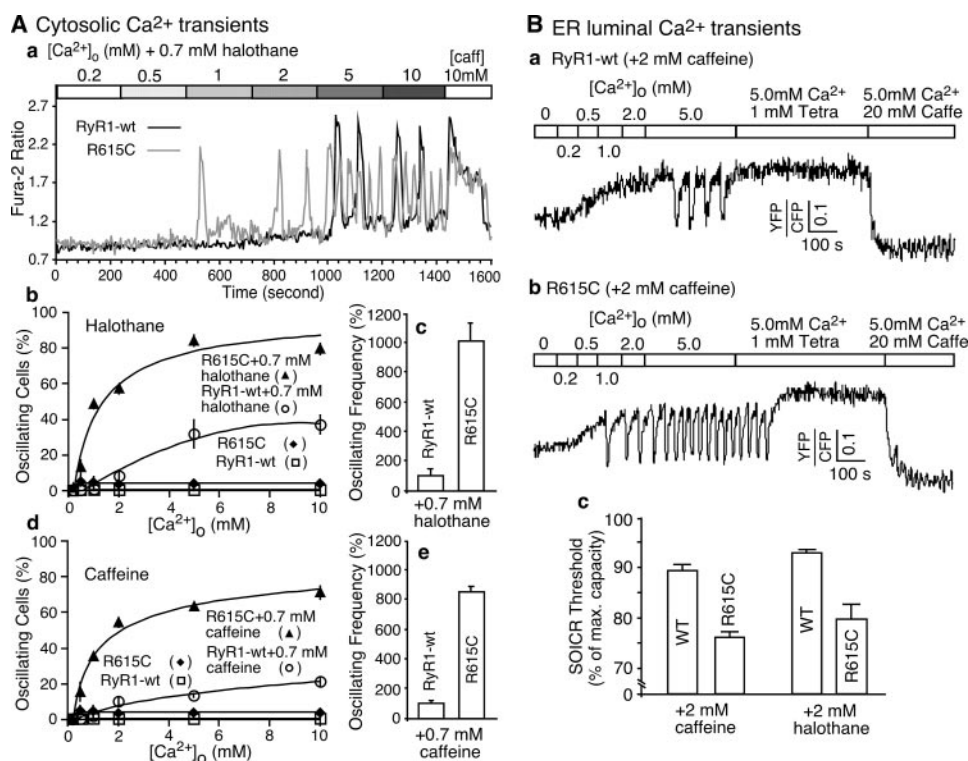
FIGURE 3. **Halothane and the MH R615C mutation increase the propensity for SOICR.** *A*, stable, inducible HEK293 cells expressing RyR1 wt and the R615C mutant were induced with tetracycline for ~24 h and loaded with 5 μM fura-2 AM in KRH buffer for 20 min at room temperature. The cells were continuously perfused with KRH buffer containing various concentrations of external Ca^{2+} (0.2–10 mM) and caffeine. *Panel a* shows single cell fluorescent Ca^{2+} images of cells expressing RyR1 wt (*top panels*) and the R615C mutant (*bottom panels*) in the presence of 0.7 mM halothane at various $[Ca^{2+}]_o$. Fura-2 ratios of representative RyR1 wt (*green trace*) and the R615C mutant (*red trace*) cells are shown in *panel b*. The fraction (%, means ± S.E.) of cells displaying Ca^{2+} oscillations in the presence or absence of 0.7 mM halothane (*panel c*) or 0.7 mM caffeine (*panel d*) is shown. The total numbers of RyR1 wt cells analyzed for Ca^{2+} oscillations were 320 (without halothane or caffeine), 465 (with 0.7 mM halothane), and 305 (with 0.7 mM caffeine). The total numbers of R615C cells analyzed for Ca^{2+} oscillations were 290 (without halothane or caffeine), 714 (with 0.7 mM halothane), and 339 (with 0.7 mM caffeine). *Panels c* and *e* show the frequency of Ca^{2+} oscillations at 2 mM $[Ca^{2+}]_o$, in the presence of 0.7 mM halothane and 0.7 mM caffeine, respectively. The values were normalized to the wt level (100%). The data shown are the means ± S.E. from three to five separate experiments. *B*, the R615C mutation decreases the threshold for SOICR. HEK293 cells expressing wt or R615C were transfected with D1ER cDNA ~48 h before imaging, and RyR1 expression was induced ~24 h before imaging. The cells were perfused with KRH buffer containing 2 mM caffeine or 2 mM halothane with various $[Ca^{2+}]_o$, 1 mM tetracaine, or 20 mM caffeine. Representative FRET traces from HEK293 cells expressing either wt (*panel a*) or R615C (*panel b*) are shown. The SOICR threshold in cells expressing wt or R615C in the presence of caffeine or halothane is shown in *panel c*. The threshold for SOICR was determined by calculating the peak luminal Ca^{2+} level during oscillations as the percentage of the maximum luminal Ca^{2+} store capacity. The maximum luminal Ca^{2+} store capacity was estimated by calculating the difference between the maximum luminal Ca^{2+} level in the presence of tetracaine (1 mM) and the minimum luminal Ca^{2+} level in the presence of caffeine (20 mM). The data shown are means ± S.E. from two to five separate experiments.

To determine whether dantrolene can also suppress caffeine-induced spontaneous Ca^{2+} release in a nonmuscle environment, we assessed the impact of dantrolene on SOICR in HEK293 cells. As shown in Fig. 4, HEK293 cells expressing the RyR1-R615C mutant exhibited Ca^{2+} oscillations in the presence of 5 mM $[Ca^{2+}]_o$ plus 2.0 mM caffeine. The addition of 100 nM dantrolene diminished these oscillations, reducing the number of oscillating cells by ~80% (Fig. 4, *A* and *B*). Fig. 4*C* shows that dantrolene suppressed SOICR in HEK293 cells expressing either the R615C mutant or RyR1 wt with an IC_{50} of ~10–20 nM. Interestingly and in contrast, dantrolene did not abolish Ca^{2+} oscillations in HEK293 cells expressing the disease-causing RyR2 mutation, N4104K, even at high concentrations (10 μM) (Fig. 4*D*). These data demonstrate that dantrolene

potently suppresses RyR1-mediated, but not RyR2-mediated, SOICR in HEK293 cells and therefore suggest that the inhibition of RyR1-mediated SOICR may represent a primary therapeutic action of dantrolene.

DISCUSSION

Investigations over the past decades have greatly advanced our understanding of the molecular and cellular mechanisms of MH. However, some fundamental questions still remain, including: 1) what intrinsic properties of the RyR1 channel altered by mutations are principally responsible for MH pathogenesis? 2) how do volatile anesthetics trigger MH? and 3) how does dantrolene suppress MH? In the present study, we demonstrated that both the MH R615C mutation and MH-triggering agent, halothane, sensitize the RyR1 channel to activation by luminal Ca^{2+} and reduce the threshold for SOICR. In contrast, dantrolene, an effective treatment for MH, suppresses SOICR. Based on these observations, we propose that volatile anesthetics, by further reducing the already reduced threshold for SOICR in the MHS muscle, trigger spontaneous Ca^{2+} release and thus MH, whereas dantrolene suppresses spontaneous Ca^{2+} release and MH by increasing the SOICR threshold.

The MH R615C Mutation Sensitizes the RyR1 Channel to Luminal Ca^{2+} Activation—Despite the consistent observation that the MHS pig RyR1 channel is more active than the normal RyR1 channel upon

stimulation, many studies have failed to detect major changes in the intrinsic sensitivity of the MHS RyR1 channel to cytosolic Ca^{2+} activation (1, 13, 15, 16, 19, 20). Consistent with these previous observations, we observed little effect of the MH R615C mutation on the cytosolic Ca^{2+} dependence of single RyR1 channels (Fig. 1*B*). How then do the MHS and normal RyR1 channels with similar intrinsic sensitivities to cytosolic Ca^{2+} activation respond so differently to activation by various stimuli? Given the importance of luminal Ca^{2+} in regulating SR Ca^{2+} release, we reasoned that MH mutations may alter the response of the RyR1 channel to luminal Ca^{2+}. To address this possibility, in the present study, we directly assessed the impact of the MH R615C mutation on the sensitivity of single RyR1 channels to luminal Ca^{2+} activation. We found that the MH
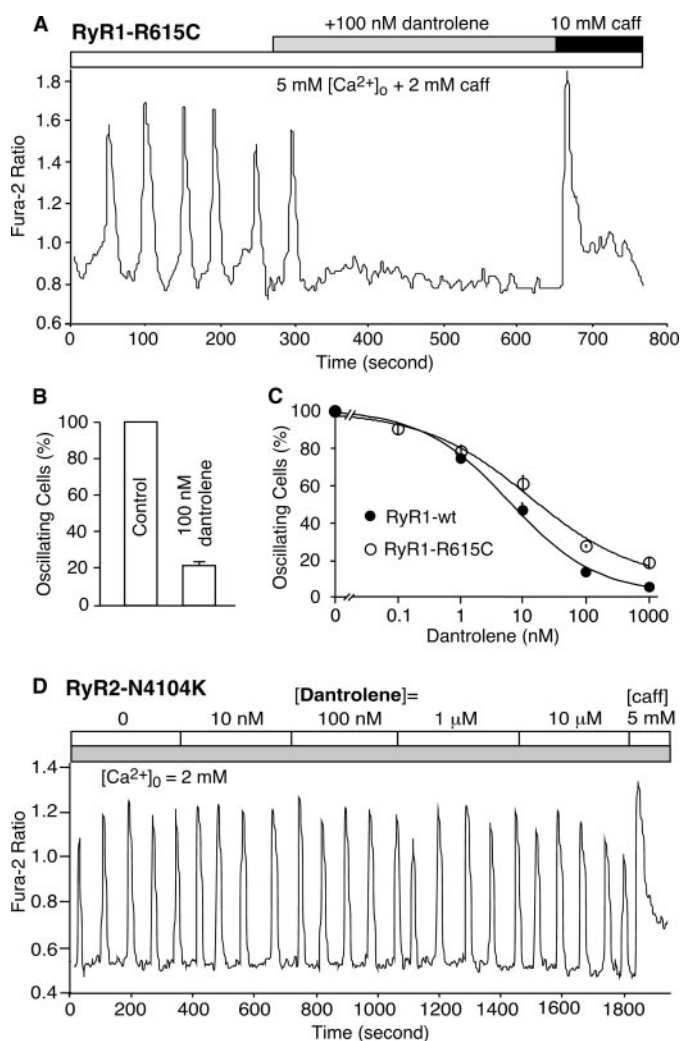
FIGURE 4. **Effect of dantrolene on SOICR.** Stable, inducible HEK293 cells expressing the RyR1-R615C mutant were loaded with fura-2 AM and perfused with KRH buffer containing 5 mM $[Ca^{2+}]_o$ plus 2 mM caffeine in the absence or the presence of 100 nM dantrolene (*A*). The fraction (%, means ± S.E.) of cells that displayed Ca^{2+} oscillations before (control) and after the addition of 100 nM dantrolene is shown in *B*. The dose dependence of dantrolene inhibition of SOICR in HEK293 cells expressing R615C (*open circles*) or expressing RyR1 wt (*solid circles*) is shown in *C*. The total numbers of cells analyzed were 706 in *B* and 366 for RyR1 wt and 260 for R615C in *C* from five to eight separate experiments. *D* shows the effect of dantrolene on SOICR in HEK293 cells expressing the disease-linked RyR2 mutant, N4104K. The cells were perfused with 2 mM $[Ca^{2+}]_o$ in the presence of 10 nM to 10 μM dantrolene (*D*). Similar results were obtained from four separate experiments.

R615C mutation markedly enhanced the luminal Ca^{2+} activation of RyR1 (Fig. 1*A*) and that halothane potentiated this response (Fig. 2). These results therefore suggest that an enhanced sensitivity of the RyR1 channel to luminal Ca^{2+} may be a primary defect resulting from the R615C mutation and contribute to the observed enhanced activity.

It remains, however, to be determined how the R615C mutation, which is located in the cytoplasmic domain of the channel, affects luminal Ca^{2+} activation. It has been proposed that the MH R615C mutation weakens the interactions between the N-terminal and the central domains and consequently destabilizes the closed state of the channel (20). It is possible that these domain-domain interactions are involved in the activation of

the channel by luminal Ca^{2+} and that weakening these interactions facilitates luminal Ca^{2+} activation.

The R615C Mutation and Halothane Reduce the Threshold for SOICR—Because SOICR is triggered by the luminal Ca^{2+} activation of RyR, an enhanced luminal Ca^{2+} response would lead to an increased propensity for SOICR. In line with this, we found that halothane and caffeine enhanced SOICR in HEK293 cells expressing the RyR1 wt or the R615C mutant (Fig. 3*A*) and that HEK293 cells expressing the R615C mutant displayed a reduced threshold for SOICR compared with cells expressing RyR1 wt (Fig. 3*B*). Consistent with these observations, a number of human MH RyR1 mutations have also been shown to increase the incidence of spontaneous Ca^{2+} release when expressed in dyspedic myotubes (39). Hence, an enhanced propensity for SOICR may be a common defect of MH RyR1 mutations.

Our observations are also consistent with the results of early studies of the MHS and normal pig skeletal muscles. Nelson *et al.* (33) demonstrated that halothane induced spontaneous contracture in MHS muscle, but not in normal muscle, and that this halothane-induced contracture is dependent on the external Ca^{2+} concentration. Nelson *et al.* (13, 24, 25) also showed that the threshold amount of SR Ca^{2+} load required for Ca^{2+}-induced Ca^{2+} release to occur in MHS pig SR vesicles was lower than that in normal pig SR and that halothane lowered this threshold. These observations have led to the proposal that a defect in some intraluminal regulatory site for Ca^{2+} release may underlie MH. Notably, these observations preceded the cloning of the RyR1 cDNA and the identification of the porcine MH mutation R615C. Similarly, Ohnishi *et al.* (34) demonstrated that the SR Ca^{2+} content required for halothane-induced Ca^{2+} release in MHS pig SR was also lower than that in normal SR. Interestingly, when the SR Ca^{2+} load was below the threshold level, halothane was unable to induce Ca^{2+} release from either normal or MHS SR vesicles (34). Consistent with these observations, we found that the activation of single RyR1 channels by halothane was also dependent on luminal Ca^{2+} (Fig. 2) and that halothane and caffeine increased the propensity for SOICR. Taken together, the results of our single channel and SOICR studies and those of previous SR Ca^{2+} release studies suggest that a reduced threshold for SOICR as a result of enhanced luminal Ca^{2+} activation of RyR1 underlies a causal mechanism of MH.

Suppression of SOICR Is a Primary Action of Dantrolene—Dantrolene, an effective treatment for MH, markedly suppresses spontaneous muscle contracture and SR Ca^{2+} release (36, 37). Despite its remarkable impact on MH, dantrolene up to ~50 μM only partially inhibits voltage- or Ca^{2+}-induced SR Ca^{2+} release, suggesting that the primary action of dantrolene is unlikely to lie in the suppression of voltage- or Ca^{2+}-induced SR Ca^{2+} release (40–42). On the other hand, if enhanced SOICR activity caused by a reduced SOICR threshold is the cause of MH, one would expect that dantrolene at clinically relevant concentrations (1–10 μM) would be able to diminish RyR1-mediated SOICR activity even in a nonmuscle environment. Indeed, we found that dantrolene inhibited SOICR in HEK293 nonmuscle cells expressing the R615C mutant with an IC_{50} of ~20 nM (Fig. 4). Similarly, Zhang *et al.* (43) have recently

shown that azumolene, a dantrolene analog, decreased the frequency of spontaneous Ca^{2+} sparks in skeletal muscle fibers with an IC_{50} of ~250 nM. The fact that much lower concentrations of dantrolene are required for suppressing RyR1-mediated SOICR compared with those required for inhibiting voltage-triggered SR Ca^{2+} release suggests that the suppression of RyR1-mediated SOICR may be a primary action of dantrolene.

Whether direct and specific binding of dantrolene to the RyR1 channel fully accounts for its therapeutic actions as a skeletal muscle relaxant and antidote for MH remains an open question (44–46). In this regard, we were unable to detect significant effects of dantrolene on either the cytosolic or luminal Ca^{2+} activation of single RyR1 channels incorporated into lipid bilayers (not shown), despite the marked effects of dantrolene on RyR1-mediated SOICR that we observed. The reasons for this apparent discrepancy are unknown. It has been shown that dantrolene binds to the N-terminal region of RyR1 and stabilizes domain-domain interactions, indicating that RyR1 or its complex is a direct target of dantrolene (47, 48). However, the functional manifestation of dantrolene binding to RyR1 may require the presence of other factors such as calmodulin, ATP, or other RyR1-associated proteins (41, 42). Importantly, we found that dantrolene did not affect SOICR in cells expressing a mutant RyR2 channel (Fig. 4). Thus our results convincingly demonstrate that dantrolene suppression of SOICR is strictly dependent on the expression of the RyR1 isoform. It has recently been shown that RyR1 is associated with components of the store-operated Ca^{2+} entry pathway and that azumolene suppresses the store-operated Ca^{2+} entry pathway that is coupled to RyR1 (49, 50). It is therefore possible that the interaction between RyR1 and components of store-operated Ca^{2+} entry pathway or other unknown RyR1-associated proteins is required for the action of dantrolene. Clearly, further studies are needed to understand the molecular mechanism by which dantrolene suppresses SOICR.

A New View of MH—Our results support a model in which the MH R615C mutation and the MH-triggering agent halothane reduce the threshold for luminal Ca^{2+} activation of RyR1 and thus the threshold for SOICR, whereas the MH-suppressing agent, dantrolene, inhibits SOICR (Fig. 5). In this view, the threshold for SOICR from normal SR is higher than the SR-free Ca^{2+} level under both resting and stimulated conditions (Fig. 5A). Therefore, there is little or no Ca^{2+} spillover from normal SR. On the other hand, in the MHS SR, the threshold for SOICR is reduced because of mutations in RyR1 (Fig. 5B). Under resting conditions, the reduced threshold for mutant channels remains higher than the resting SR-free Ca^{2+} level, so that there is again little or no Ca^{2+} spillover. However, in the presence of MH-triggering agents (*e.g.* halothane), the threshold is further reduced, and SOICR is more likely to occur. The resulting SR Ca^{2+} spillover leads to spontaneous muscle contraction and MH. Dantrolene reverses the effect of the MH mutations and of volatile anesthetics by increasing the SOICR threshold.

In this working model, SR Ca^{2+} handling in MHS muscles at rest is expected to be normal, if the reduced SOICR threshold would still be significantly higher than the resting SR-free Ca^{2+} level. Consistent with this prediction, the majority of MHS individuals are asymptomatic in the absence of triggering agents.
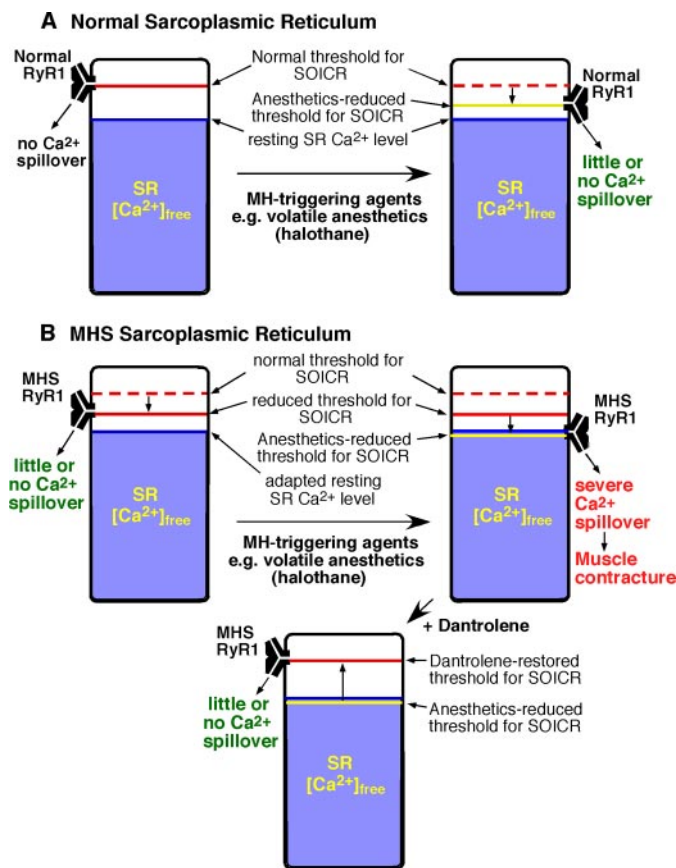

FIGURE 5. **A proposed model for the action of the porcine MH mutation, the MH-triggering agent, halothane, and the MH-suppressing agent, dantrolene.** The threshold for SOICR and the SR-free Ca^{2+} level in normal (*A*) and the MHS SR (*B*) in the resting and stimulated states are schematically shown. The SOICR threshold, which is reduced in the MHS SR as a consequence of the R615C RyR1 mutation (*short arrow*), is depicted by a *red bar*. The SR-free Ca^{2+} level is represented by the *blue area*. The anesthetic-reduced SOICR threshold is depicted by a *yellow bar*. When the SOICR threshold decreases to the SR-free Ca^{2+} level, SOICR occurs, leading to a large SR Ca^{2+} spillover, which can trigger spontaneous Ca^{2+} release, muscle contraction, and MH. Dantrolene restores the reduced SOICR threshold.

However, if the reduced SOICR threshold were too close to the resting SR Ca^{2+} level because of more severe RyR1 mutations, Ca^{2+} spillover could occur even under the resting conditions. Such uncontrolled SR Ca^{2+} release at rest may account for the muscle defects seen in those MHS individuals with central core disease (1–5).

Implication for Stress-induced MH—In addition to volatile anesthetics, physical and emotional stress can also trigger MH in pigs and humans, but the mechanism underlying stress-induced MH is unclear. It is well known that in the heart, physical and emotional stress activates the β-adrenergic receptor/cAMP/cAMP-dependent protein kinase signaling pathway, leading to an increase in the SR Ca^{2+} load and SR Ca^{2+} release (51). Rudolf *et al.* (52) have recently demonstrated directly that, as in cardiac muscle, β-adrenergic receptor stimulation also increases the SR Ca^{2+} load and Ca^{2+} release in skeletal muscle. Because the occurrence of SOICR is determined not only by its threshold but also by the SR Ca^{2+} load (Fig. 5), physical and emotional stress may induce SOICR by increasing the SR Ca^{2+} load. Because the threshold for SOICR is reduced in the MHS SR, SOICR and thus spontaneous muscle

contraction would be more likely to occur in MHS pigs or individuals during stress-induced SR Ca^{2+} overload. Therefore, conditions that affect either the SOICR threshold or SR Ca^{2+} loading will have a profound impact on the occurrence of SOICR and thus the susceptibility to MH. This multi-factorial dependence of the occurrence of SOICR may provide an explanation for the unsolved heterogeneity of MH expression in MHS individuals carrying even the same RyR1 mutation.

Conclusions—In summary, the present study sheds novel insight into the causal mechanism of MH and proposes a unifying model for MH susceptibility, MH triggering, and MH suppression. We have demonstrated that both the MH R615C mutation and the MH trigger halothane act to reduce the threshold for luminal Ca^{2+} activation and SOICR, whereas the MH antidote dantrolene suppresses SOICR. Together these data suggest that the sensitivity of the RyR1 channel to luminal Ca^{2+} activation plays a central role in the pathogenesis of MH.

REFERENCES

1. Mickelson, J. R., and Louis, C. F. (1996) *Physiol. Rev.* **76,** 537–592
2. Loke, J., and MacLennan, D. H. (1998) *Am. J. Med.* **104,** 470–486
3. McCarthy, T. V., Quane, K. A., and Lynch, P. J. (2000) *Hum. Mutat.* **15,** 410–417
4. Lyfenko, A. D., Goonasekera, S. A., and Dirksen, R. T. (2004) *Biochem. Biophys. Res. Commun.* **322,** 1256–1266
5. Treves, S., Anderson, A. A., Ducreux, S., Divet, A., Bleunven, C., Grasso, C., Paesante, S., and Zorzato, F. (2005) *Neuromuscul. Disord.* **15,** 577–587
6. Fujii, J., Otsu, K., Zorzato, F., de Leon, S., Khanna, V. K., Weiler, J. E., O'Brien, P. J., and MacLennan, D. H. (1991) *Science* **253,** 448–451
7. MacLennan, D. H., and Phillips, M. S. (1992) *Science* **256,** 789–794
8. Robinson, R., Carpenter, D., Shaw, M., Halsall, J., and Hopkins, P. (2006) *Hum. Mutat.* **27,** 977–989
9. Otsu, K., Nishida, K., Kimura, Y., Kuzuya, T., Hori, M., Kamada, T., and Tada, M. (1994) *J. Biol. Chem.* **269,** 9413–9415
10. Treves, S., Larini, F., Menegazzi, P., Steinberg, T. H., Koval, M., Vilsen, B., Andersen, J. P., and Zorzato, F. (1994) *Biochem. J.* **301,** 661–665
11. Tong, J., Oyamada, H., Demaurex, N., Grinstein, S., McCarthy, T. V., and MacLennan, D. H. (1997) *J. Biol. Chem.* **272,** 26332–26339
12. Dietze, B., Henke, J., Eichinger, H. M., Lehmann-Horn, F., and Melzer, W. (2000) *J. Physiol. (Lond.)* **526,** 507–514
13. Nelson, T. E. (2002) *Curr. Mol. Med.* **2,** 347–369
14. Yang, T., Ta, T. A., Pessah, I. N., and Allen, P. D. (2003) *J. Biol. Chem.* **278,** 25722–25730
15. Fill, M., Coronado, R., Mickelson, J. R., Vilven, J., Ma, J. J., Jacobson, B. A., and Louis, C. F. (1990) *Biophys. J.* **57,** 471–475
16. Shomer, N. H., Louis, C. F., Fill, M., Litterer, L. A., and Mickelson, J. R. (1993) *Am. J. Physiol.* **264,** C125–C135
17. Laver, D. R., Owen, V. J., Junankar, P. R., Taske, N. L., Dulhunty, A. F., and Lamb, G. D. (1997) *Biophys. J.* **73,** 1913–1924
18. Owen, V. J., Taske, N. L., and Lamb, G. D. (1997) *Am. J. Physiol.* **272,** C203–C211
19. Balog, E. M., Fruen, B. R., Shomer, N. H., and Louis, C. F. (2001) *Biophys. J.* **81,** 2050–2058
20. Murayama, T., Oba, T., Hara, H., Wakebe, K., Ikemoto, N., and Ogawa, Y. (2007) *Biochem. J.* **402,** 349–357
21. Tripathy, A., and Meissner, G. (1996) *Biophys. J.* **70,** 2600–2615
22. Sitsapesan, R., and Williams, A. J. (1997) *J. Membr. Biol.* **159,** 179–185
23. Gyorke, S., and Terentyev, D. (2008) *Cardiovasc. Res.* **77,** 245–255
24. Nelson, T. E. (1983) *J. Clin. Investig.* **72,** 862–870
25. Nelson, T., Lin, M., and Volpe, P. (1991) *J. Pharmacol. Exp. Ther.* **256,** 645–649
26. Jiang, D., Xiao, B., Yang, D., Wang, R., Choi, P., Zhang, L., Cheng, H., and Chen, S. R. W. (2004) **101,** 13062–13067
27. Jiang, D., Wang, R., Xiao, B., Kong, H., Hunt, D. J., Choi, P., Zhang, L., and Chen, S. R. W. (2005) *Circ. Res.* **97,** 1173–1181
28. Priori, S. G., and Napolitano, C. (2005) *J. Clin. Investig.* **115,** 2033–2038
29. Ho, S. N., Hunt, H. D., Horton, R. M., Pullen, J. K., and Pease, L. R. (1989) *Gene (Amst.)* **77,** 51–59
30. Fabiato, A., and Fabiato, F. (1979) *J. Physiol. (Paris)* **75,** 463–505
31. Palmer, A. E., Jin, C., Reed, J. C., and Tsien, R. Y. (2004) *Proc. Natl. Acad. Sci. U. S. A.* **101,** 17404–17409
32. Housmans, P. R., and Wanek, L. A. (2000) *Anal. Biochem.* **284,** 60–64
33. Nelson, T. E., Bedell, D. M., and Jones, E. W. (1975) *Anesthesiology* **42,** 301–306
34. Ohnishi, S. T., Taylor, S., and Gronert, G. A. (1983) *FEBS Lett.* **161,** 103–117
35. Tong, J., Du, G. G., Chen, S. R., and MacLennan, D. H. (1999) *Biochem. J.* **343,** 39–44
36. Okumura, F., Crocker, B. D., and Denborough, M. A. (1980) *Br. J. Anaesth.* **52,** 377–383
37. Foster, P. S., and Denborough, M. A. (1989) *Br. J. Anaesth.* **62,** 566–572
38. Van Winkle, W. B. (1976) *Science* **193,** 1130–1131
39. Dirksen, R. T., and Avila, G. (2004) *Biophys. J.* **87,** 3193–3204
40. Hainaut, K., and Desmedt, J. (1974) *Nature* **252,** 728–730
41. Fruen, B. R., Mickelson, J. R., and Louis, C. F. (1997) *J. Biol. Chem.* **272,** 26965–26971
42. Louis, C., Balog, E., and Fruen, B. (2001) *Biosci. Rep.* **21,** 155–168
43. Zhang, Y., Rodney, G. G., and Schneider, M. F. (2005) *J. Pharmacol. Exp. Ther.* **314,** 94–102
44. Nelson, T., Lin, M., Zapata-Sudo, G., and Sudo, R. (1996) *Anesthesiology* **84,** 1368–1379
45. Szentesi, P., Collet, C., Sarkozi, S., Szegedi, C., Jona, I., Jacquemond, V., Kovacs, L., and Csernoch, L. (2001) *J. Gen. Physiol.* **118,** 355–375
46. Cherednichenko, G., Ward, C. W., Feng, W., Cabrales, E., Michaelson, L., Samso, M., Lopez, J. R., Allen, P. D., and Pessah, I. N. (2008) *Mol. Pharmacol.* **73,** 1203–1212
47. Paul-Pletzer, K., Yamamoto, T., Bhat, M. B., Ma, J., Ikemoto, N., Jimenez, L. S., Morimoto, H., Williams, P. G., and Parness, J. (2002) *J. Biol. Chem.* **277,** 34918–34923
48. Kobayashi, S., Bannister, M. L., Gangopadhyay, J. P., Hamada, T., Parness, J., and Ikemoto, N. (2005) *J. Biol. Chem.* **280,** 6580–6587
49. Sampieri, A., Diaz-Munoz, M., Antaramian, A., and Vaca, L. (2005) *J. Biol. Chem.* **280,** 24804–24815
50. Zhao, X., Weisleder, N., Han, X., Pan, Z., Parness, J., Brotto, M., and Ma, J. (2006) *J. Biol. Chem.* **281,** 33477–33486
51. Bers, D. M. (2002) *Nature* **415,** 198–205
52. Rudolf, R., Magalhaes, P. J., and Pozzan, T. (2006) *J. Cell Biol.* **173,** 187–193